Inorganic Chemistry

Article

pubs.acs.org/IC

Tris Chelating Phosphate Complexes of Bis(thio)urea Ligands

Rui Li,[†,§] Yanxia Zhao,[†,§] Shaoguang Li,[†] Peiju Yang,[†] Xiaojuan Huang,[†] Xiao-Juan Yang,[†,‡] and Biao Wu*[,‡]

[†]State Key Laboratory for Oxo Synthesis & Selective Oxidation, Lanzhou Institute of Chemical Physics, CAS, Lanzhou 730000, China

[‡]Key Laboratory of Synthetic and Natural Functional Molecule Chemistry of the Ministry of Education, College of Chemistry and Materials Science, Northwest University, Xi'an 710069, China

[§]Graduate University of Chinese Academy of Sciences, Beijing 100049, China

Supporting Information

ABSTRACT: Two bisurea (L^1, L^2) and one bisthiourea (L^3) ligands were synthesized and their anion coordination behavior was studied. These ligands can readily form the tris chelates $[PO_4(L)_3]^{3-}$ (**1**, **5**, and **6**) with phosphate ion (PO_4^{3-}) in the solid state, in which the anion is coordinated by six urea groups through 12 hydrogen bonds. Solution binding studies by ^1H NMR and UV−vis spectroscopy revealed different binding properties of the ligands toward phosphate ion. While the bis(*p*-nitrophenyl)-substituted bisurea L^1 retains the 3:1 (host to guest) binding ratio in solution, the diethyl derivative L^2 only forms 1:1 complex with phosphate ion. The more acidic thiourea L^3 undergoes deprotonation/decomposition in the presence of phosphate ion. Moreover, the sulfate complex (**2**) of L^1 and bicarbonate (**3**) and carbonate (**4**) complexes of L^2 have also been obtained, which show lower coordination numbers both in the solid state and in solution.

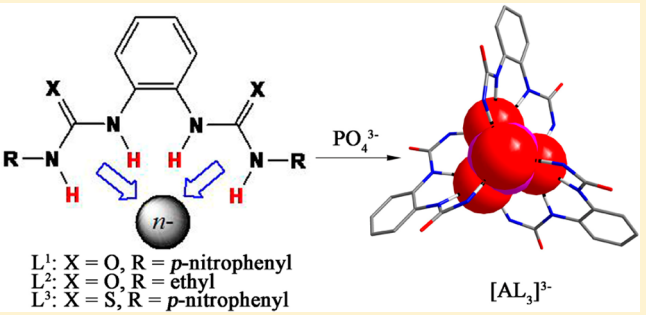

INTRODUCTION

The supramolecular chemistry of anions is an important area because of the crucial relevance of anions in a range of biological, chemical, medical, and environmental processes.[1] In 1967, Park and Simmons reported the encapsulation of chloride ion inside the cavity of bicyclic diammonium receptors, which were essentially the first anion complexes.[1] On the basis of the research of cyclic ammonium hosts with halide anions, Lehn first proposed the concept of anion coordination in 1978.[2] This field has attracted much attention in recent years, and it has been found that anion complexes also exhibit "double valence" as transition metal complexes: anions act as the "primary valence" while hydrogen bonds between the receptor and anion provide a "coordination number", acting as the "secondary valence".[3] Subsequently, anions also require coordination saturation and geometrical preference, although such features are not as well-defined as in transition metal coordination. These similarities not only open a new window to the theoretical development of anion coordination chemistry, but also shed light on the design of anion ligands.

In transition-metal coordination chemistry, bidentate chelating ligands (e.g., 2,2′-bipyridine, bpy) are widely used in the construction of coordination and supramolecular compounds.[4] For octahedral metal ions, an interesting class of molecules (the tris chelates) which have a metal ion coordinated by three bidentate ligands can readily form. In particular, the tris chelating bpy complexes $[M(bpy)_3]^{n+}$ display remarkable chemical and physical properties and have thus been extensively investigated in helical assembly,[5] chiral molecular recognition,[6] luminescent devices,[7] and applications in photonics and optoelectronics[8] and electrochemistry.[9]

Recently our research has focused on anion coordination chemistry of urea-based ligands.[10] A series of *ortho*-phenylene bridged oligoureas, which display excellent coordination abilities to the tetrahedral sulfate and phosphate anions, have been designed by mimicking the well-known oligopyridine ligands. The tris(urea) ligands[10c] are highly complementary for PO_4^{3-} ion in the complexes $[(PO_4)L_2]^{3-}$ (Scheme 2a, right), which closely resemble the metal-terpyridine complexes

Scheme 1. Structures of the Ligands L^1, L^2, and L^3

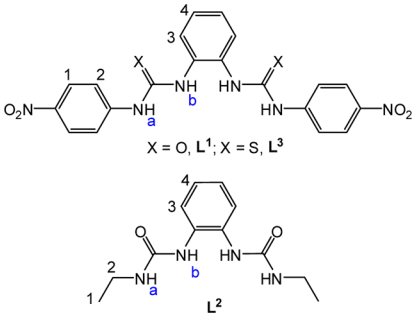

Received: December 20, 2012

   dx.doi.org/10.1021/ic3028012 | *Inorg. Chem.* XXXX, XXX, XXX−XXX

Scheme 2. Design of the Trisurea and Bisurea Ligands by Mimicking the Terpyridine (tpy) and Bipyridine (bpy) Moieties (a) $[M(tpy)_2]^{n+}$ and $[A(trisurea)_2]^{3-}$;[10c] and (b) $[M(bpy)_3]^{n+}$ and $[A(bisurea)_3]^{3-}$ (A = PO_4^{3-})

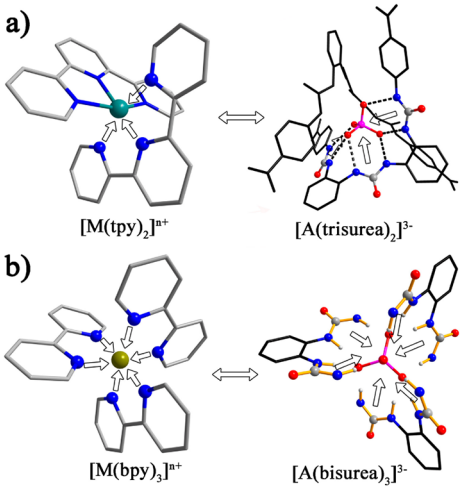

$[M(tpy)_2]^{n+}$ (Scheme 2a, left). Moreover, a bis-bisurea ligand[10g] assembles with phosphate to form the first triple-stranded anion helicate, exactly as in the case of bis-bidentate ligands and metal ions. In these anion complexes, the phosphate ion (PO_4^{3-}) displays a strong tendency for coordination saturation (12 hydrogen bonds or six urea groups). Therefore, we turned to the bisurea ligands which should form the $[AL_3]$-type (A = anion) complexes with phosphate ion like the famous metal-bpy counterpart $[M(bpy)_3]^{n+}$. Indeed, some *ortho*-phenylene bridged bisurea receptors (and related NH-based receptors)[11] have been synthesized, and their binding properties toward various anions, such as F^-, Cl^-, $H_2PO_4^-$, SO_4^{2-}, CN^-, NO_3^-, $RCOO^-$, have been examined. However, studies on the binding of the fully deprotonated PO_4^{3-} anion are very rare. Very recently, Gale et al.[12] reported a phosphate (PO_4^{3-}) complex with three 1,3-diindolylurea ligands. In this present work, we synthesized three bis(thio)urea ligands ($\mathbf{L^1}$–$\mathbf{L^3}$; Scheme 1), which can readily coordinate with PO_4^{3-} ion to form the desired "trischelate" $[(PO_4)L_3]^{3-}$ complexes (**1**, **5**, **6**). In addition, a sulfate complex (**2**) with $\mathbf{L^1}$, bicarbonate complex (**3**) and carbonate complex (**4**) with $\mathbf{L^2}$ were also obtained in the solid state. Herein, we describe the synthesis and structures of these anion complexes, as well as the coordination behavior of $\mathbf{L^1}$, $\mathbf{L^2}$, and $\mathbf{L^3}$ with a variety of oxo anions in solution.

RESULTS AND DISCUSSION

Synthesis. The nitrophenyl-decorated bisurea ligand $\mathbf{L^1}$ was prepared according to the literature procedures.[13] The ethyl-substituted ligand $\mathbf{L^2}$ and the thiourea $\mathbf{L^3}$ were synthesized by the reaction of *o*-phenylenediamine with ethyl isocyanate or *p*-nitrophenylisothiocyanate, respectively, as white and yellow powders. The anion complexes **1**–**6** were synthesized by reaction of the ligands with different salts of the anions. Treatment of $\mathbf{L^1}$, $\mathbf{L^2}$, or $\mathbf{L^3}$ with phosphate salts afforded the $[(PO_4)L_3]^{3-}$complexes **1**, **5**, and **6**, which consist of three ligands and one PO_4^{3-} coordinated by 12 hydrogen bonds. The sulfate complex $[K([18]crown\text{-}6)]_2[SO_4(\mathbf{L^1})_2]\cdot C_3H_6O$ (**2**), which contains two ligand molecules coordinating to a sulfate ion, was obtained from $\mathbf{L^1}$, K_2SO_4, and [18]crown-6. Interestingly, an unexpected 1:1 bicarbonate complex, $[K([18]crown\text{-}6)]\cdot[(HCO_3)(\mathbf{L^2})]$ (**3**), was isolated from $\mathbf{L^2}$, [18]-crown-6, and K_3PO_4. However, when $\mathbf{L^2}$ was treated with $(TEA)HCO_3$ (TEA = tetraethylammonium), a complex with the deprotonated carbonate ion, $(TEA)_2[(CO_3)(\mathbf{L^2})_2]$ (**4**), was obtained.

Crystal Structures. *Ligand L^1 and Its Complexes.* First, the symmetric bisurea ligand $\mathbf{L^1}$ with two *p*-nitrophenyl groups as pendants was employed, whose electron withdrawing property makes the urea groups more acidic and thus can ensure effective coordination with anions. Single crystals of the free ligand $\mathbf{L^1}$ were obtained through evaporation of a solution in acetone–DMSO (v/v 20:1) at room temperature. In the crystal structure, one of the *p*-nitrophenyl-urea arms is roughly coplanar with the *o*-phenylene bridge (dihedral angle 12°), while the other arylurea plane is nearly perpendicular to the *o*-phenylene ring (dihedral angle 77°). The urea group on the perpendicular arm uses the carbonyl oxygen to form the typical six-membered hydrogen bonds (N2···O4, 2.900 Å; N3···O4, 3.062 Å; Figure S1, Supporting Information) with the NH groups of the other urea arm in an adjacent ligand and binds with a DMSO molecule via two hydrogen bonds (N4···O7, 2.916 Å; N5···O7, 2.877 Å; Figure S1), leading to an infinite 1D tape.

Phosphate Complex $[K([18]crown\text{-}6)]_2(TBP)[PO_4(L^1)_3]$ (1). The coordination of phosphate ion with ligand $\mathbf{L^1}$ was studied by using different phosphate salts. Note that attempts to grow crystals of the phosphate complex with various countercations, such as TBA^+ (TBA^+ = tetrabutylammonium), TBP^+ (TBP^+ = tetrabutylphosphonium), $[K([18]crown\text{-}6)]^+$, K^+, and Na^+, were unsuccessful. Interestingly, when two mixed countercations ($[K([18]crown\text{-}6)]^+$ and TBP^+) were present, yellow block single crystals of the tris-chelating complex **1** were obtained with the composition $[K([18]crown\text{-}6)]_2(TBP)[PO_4(\mathbf{L^1})_3]$.

The crystal structure clearly shows that a phosphate ion is coordinated by three ligands via 12 hydrogen bonds from six urea groups. Notably, the three receptors around the phosphate ion are not C_3-symmetric, displaying two different coordination manners. Four urea groups from two ligands (green and blue, Figure 1a) bind four edges of the tetrahedral anion (through eight-membered H-bonded rings), while the two urea groups

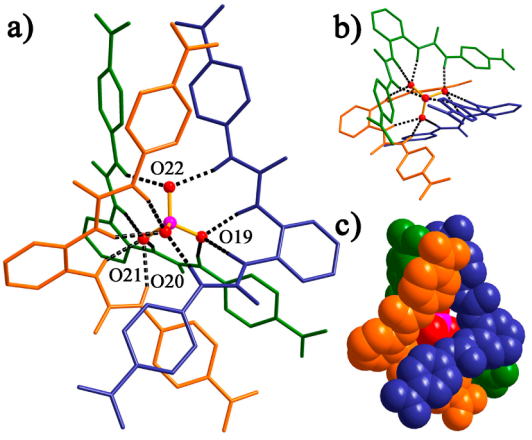

Figure 1. Crystal structure of the phosphate complex $[PO_4(\mathbf{L^1})_3]^{3-}$ (**1**). (a) Side view, (b) top view, (c) space-filling representation. Nonacidic hydrogen atoms and countercations were omitted for clarity.

dx.doi.org/10.1021/ic3028012 | Inorg. Chem. XXXX, XXX, XXX–XXX

from the third ligand (orange, Figure 1a) chelate two vertices of the phosphate ion (six-membered H-bonded rings).[14] Thus, the O19 and O20 atoms of phosphate form three hydrogen bonds each, but the O21 atom receives four and O22 only two hydrogen bonds. This is different from the complex $[(PO_4)$-$(tris\text{-}urea)_2]^{3-}$, in which all of the six urea groups chelate an edge of the tetrahedral anion and each oxygen atom forms three hydrogen bonds.[10c] The hydrogen bonds in complex **1** (N···O, 2.935−2.724 Å, 2.809 Å on average; N−H···O, 147−177°, 162° on average; Table 1) are slightly stronger than those

Table 1. Hydrogen Bond Parameters (Å, deg) around the PO_4^{3-} Ion in $[PO_4(L^1)_3]^{3-}$ (1)

N−H···O	N−H	H···O	N···O	∠NHO
N2−H2···O22	0.88	2.02	2.881(5)	164
N3−H3···O19	0.88	1.87	2.744(5)	169
N4−H4···O19	0.88	1.94	2.801(6)	165
N5−H5···O20	0.88	1.88	2.763(6)	177
N8−H8···O21	0.88	2.09	2.910(5)	155
N9−H9···O21	0.88	2.02	2.834(5)	153
N10−H10···O20	0.88	2.14	2.935(5)	151
N11−H11···O20	0.88	1.88	2.724(5)	159
N14−H14···O19	0.88	1.90	2.759(5)	166
N15−H15···O21	0.88	1.89	2.762(5)	170
N16−H16···O21	0.88	1.92	2.791(5)	170
N17−H17···O22	0.88	2.03	2.804(6)	147

in the trisurea complex (av N···O distance 2.829 Å and av N−H···O angle 164°).[10c] The expanded structure of complex **1** shows strong interactions between $[K([18]crown\text{-}6)]^+$ countercations and *p*-nitrophenyl groups, which may provide additional stability for complex **1** despite the sterical repulsion of the *p*-nitrophenyl groups.

In the literature, the binding of some anions by bisurea or analogous ligands has been described. For example, Gale et al.[15] reported a series of *o*-phenylenediamine-based bisureas which display good selectivity for carboxylate anions. Fabbrizzi et al.[16] synthesized a pair of chiral bisurea receptors and studied their affinity with dihydrogen phosphate and *D*-2,3-diphosphoglycerate anions. A phosphate (PO_4^{3-}) complex with three 1,3-diindolylureas was crystallized in the presence of excess tetrabutylammonium dihydrogen phosphate.[12] Complex **1** represents another example of tris-chelating phosphate complex which is similar to the diindolylurea complex.

*Sulfate Complex $[K([18]crown\text{-}6)]_2[SO_4(L^1)_2]$ (**2**).* The coordination of ligand $\mathbf{L^1}$ with sulfate ion was also examined. Slow diffusion of diethyl ether into an acetone solution containing $\mathbf{L^1}$, [18]crown-6, and K_2SO_4 afforded yellow crystals of the sulfate complex $[K([18]crown\text{-}6)]_2[SO_4(\mathbf{L^1})_2]\cdot C_3H_6O$ (**2**). Unlike the phosphate analogue **1**, the sulfate ion is coordinated by two bisurea molecules through eight N−H···O hydrogen bonds (N···O distances range from 2.809 to 2.972 Å, 2.890 Å on average; N−H···O angles from 153° to 170°, 161° on average; Figure 2 and Table S1, Supporting Information), which are slightly longer than those in complex **1**. The coordination sphere of the sulfate ion is further completed by one $[K([18]crown\text{-}6)]^+$ countercation, which offers two K−O bonds to two oxygen atoms of sulfate with bond lengths of 2.826 and 2.966 Å (Figure 2a). Interestingly, UV−vis and ^1H NMR titrations revealed that the 1:1 rather than 2:1 (host−guest) binding mode was formed in solution (*vide infra*).

Indeed, both the theoretical calculations[17] and X-ray crystallography[10e,18] confirmed that sulfate ion can achieve saturated coordination (12 hydrogen bonds) by six urea groups chelating the six edges of the tetrahedral anion. However, sulfate complexes with the coordination number of 6−11 have also been proven to exist in solid state and in solution.[10a,f,h,19] In some cases, the main coordination motif was supplemented by ion-pair interactions.[20a−c] Ghosh[20b] reported a tripodal urea receptor that encapsulates sulfate ion with the help of two TBA^+ countercations forming five strong C−H···O contacts. We have also obtained sulfate complexes of bis-bisurea ligands having nine N−H···O hydrogen bonds from urea groups and additional C−H···O interactions from TBA^+.[20c] In the present complex **2**, one of the $[K([18]crown\text{-}6)]^+$ countercations participates in ion-pair interaction by direct K−O bonds rather than hydrogen bonding (such as in the case of TBA^+). The different coordination modes between the phosphate complex **1** and sulfate complex **2** might be attributed to the weaker basicity and smaller charge of sulfate than phosphate ion.

*Complexes of Ligand L^2. Bicarbonate Complex $[K([18]crown\text{-}6)]\cdot[(HCO_3)(L^2)]$ (**3**).* The bisurea ligand ($\mathbf{L^2}$) with the less electron-withdrawing ethyl groups was synthesized in order to evaluate the effect of electronic properties of the bisurea ligands on their anion coordination behavior. When $\mathbf{L^2}$ was mixed with [18]crown-6 and K_3PO_4 in acetone−water (v/v 40:1), block colorless crystals were obtained upon slow vapor diffusion of diethyl ether. Unexpectedly, X-ray crystallography revealed that it is not the phosphate complex but a bicarbonate

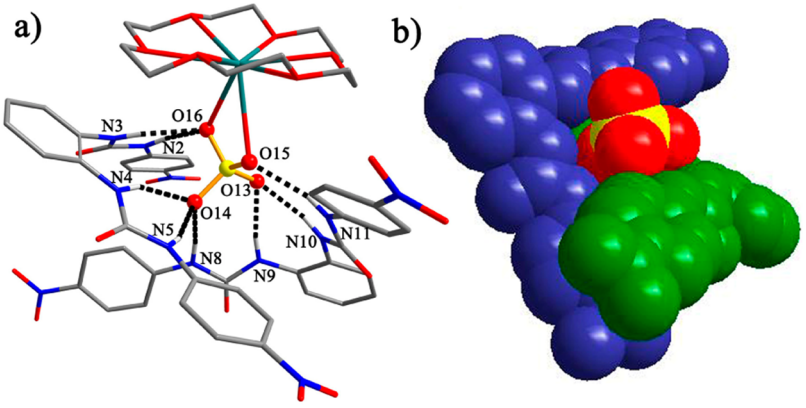

Figure 2. Crystal structure of the sulfate complex $[SO_4(\mathbf{L^1})_2]^{2-}$ (**2**). (a) The coordination sphere of sulfate ion with two $\mathbf{L^1}$ ligands and one $[K([18]crown\text{-}6)]^+$ cation. (b) Space-filling representation. Nonacidic hydrogen atoms and noninteracting countercations were omitted for clarity.

dx.doi.org/10.1021/ic3028012 | Inorg. Chem. XXXX, XXX, XXX−XXX

complex [K([18]crown-6)]·[$(HCO_3)(L^2)$] (**3**), which may result from the fixation of atmospheric CO_2 in basic solution. There are some examples of CO_3^{2-} or HCO_3^- binding originating from CO_2. Pfeffer et al.[20e] demonstrated that a naphthalimide-based thiourea can form bicarbonate adduct in the presence of tetrabutylammonium fluoride (TBAF) in DMSO. Gale et al.[20d] also showed evidence of carbonate binding with an amidourea macrocycle under similar conditions. In both cases, the source of the CO_3^{2-}/HCO_3^- was the dissolved CO_2 that was converted to carbonates. More recently, Ghosh et al.[20f] reported a neutral receptor which displayed efficient fixation of atmospheric CO_2 to carbonate ion.

In complex **3**, a bisurea molecule binds one HCO_3^- ion in its cleft through three strong hydrogen bonds (N···O, 2.813–2.979 Å; ∠N–H···O, 144–172°) and a much weaker one (N4···O7, 3.236 Å; ∠N–H···O, 143°; Figure 3a and Table S2, Supporting Information). Each urea group chelates an edge of the triangular anion. Notably, two HCO_3^- anions are associated to each other through a pair of O–H···O hydrogen bonds (O7–H7···O5: 2.643 Å, 172°) to form a $[(HCO_3)_2]^{2-}$ dimer (Figure 3a). In addition, the [K([18]crown-6)]$^+$ countercation acts as a bridge between two [$(HCO_3)(L^2)$] units, coordinating to two oxygen atoms from a urea carbonyl and a HCO_3^- ion, respectively, on its axial positions (K–O bond lengths: 2.811 and 2.744 Å). As a result, a one-dimensional "double chain" is formed with alternate [K([18]crown-6)]$^+$ ions and $[(HCO_3)_2(L^2)_2]$ moieties (Figure 3b). The presence of HCO_3^- in complex **3** was proven by the IR spectrum, which shows new peaks at 1698, 1352, 1215, 961, and 839 cm^{-1} due to the stretching and bending of HCO_3^- ion (Figure S2).[21] Moreover, ESI-MS studies also confirmed the existence of HCO_3^- ion in complex **3** by a peak at m/z = 311.1455 corresponding to [$(HCO_3)L^2$]$^-$ (calculated m/z = 311.1355).

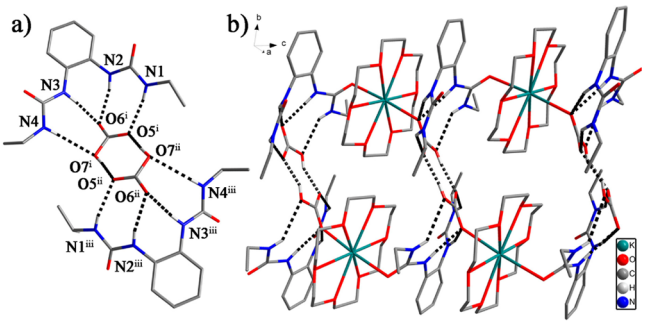

Figure 3. Crystal structure of the bicarbonate complex [$(HCO_3)L^2$]$^-$ (**3**). (a) The coordination sphere of the $[(HCO_3)_2]^{2-}$ dimer. Symmetry codes: (i) 1 + x, y, z; (ii) 1 − x, −y, 1 − z; (iii) 2 − x, −y, 1 − z. (b) part of the infinite double chain structure.

*Carbonate Complex (TEA)$_2$[$(CO_3)(L^2)_2$] (**4**).* Since the bicarbonate complex **3** was obtained by capturing the atmospheric CO_2, we attempted to repeat the synthesis by using (TEA)HCO_3 directly. However, in this case the complex (**4**) of the deprotonated anion (CO_3^{2-}) was obtained. Similar phenomena were also observed in the crystallization of (TEA)HCO_3 with a diindolylurea[12] or *m*-nitrophenyl-substituted bisurea,[15a] both of which resulted in the binding of the anion in the form of CO_3^{2-} and can be attributed to proton transfer between the bound and free anions. It should be noted that, due to the crystal-imposed inversion symmetry, the three oxygen atoms of carbonate are distributed to four positions with 0.75 occupancy rate each, forming a rhombus (Figure 4a).

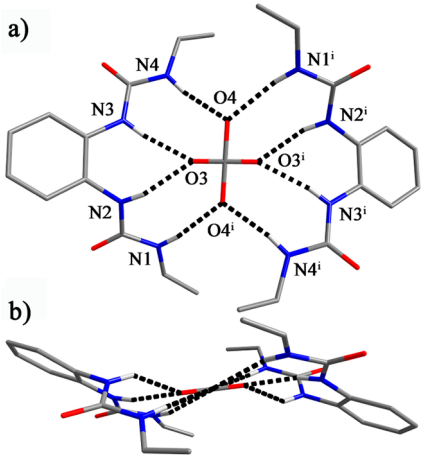

Figure 4. Crystal structure of the carbonate complex [$(CO_3)(L^2)_2$]$^{2-}$ (**4**): (a) top view; (b) side view. (Note: the three oxygen atoms of carbonate anion are distributed to four positions.) Symmetry code: (i) 1 − x, −y, 1 − z.

In contrast to the 1:1 binding of HCO_3^-, the CO_3^{2-} anion is encapsulated by two L^2 ligands in a nearly planar structure (Figure 4b). Each urea group chelates two partially occupied oxygen atoms of the anion, forming a total of eight hydrogen bonds (N···O, 2.728–2.901 Å; N–H···O, 144–167°). The existence of the CO_3^{2-} was also confirmed by the IR spectrum which shows distinct peaks at 1692 and 1372 cm^{-1} (Figure S3).[21]

*Phosphate Complex (TMA)$_3$[$PO_4(L^2)_3$]·4H_2O (**5**).* Fortunately, treatment of L^2 with $(TMA)_3PO_4$ (generated from (TMA)OH and H_3PO_4, TMA = tetramethylammonium) in acetonitrile and diethyl ether afforded rodlike colorless crystals of complex **5**, which has the composition $(TMA)_3[PO_4(L^2)_3]\cdot 4H_2O$ as confirmed by X-ray crystallographic and elemental analysis. Utilization of other countercations, such as TBA$^+$, TBP$^+$, K$^+$, and Na$^+$, failed to generate single crystals. In the structure of **5**, three L^2 ligands coordinate to one phosphate ion through six urea groups, each of which chelates an edge of the anion tetrahedron (Figure 5a). The N···O distances (2.700–2.943 Å, 2.820 Å on average; Table 2) are slightly longer than those of complex **1** but are similar to the complex of tris(urea) ligands.[10c] Notably, the two ethyl groups within each ligand adopt the *syn*-conformation relative to the *o*-

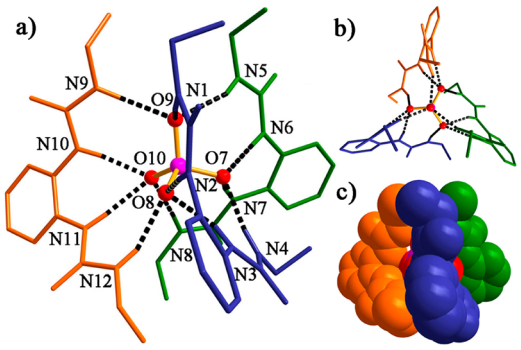

Figure 5. Crystal structure of [$PO_4(L^2)_3$]$^{3-}$ (**5**): (a) Side view; (b) top view; (c) space-filling representation.

dx.doi.org/10.1021/ic3028012 | Inorg. Chem. XXXX, XXX, XXX–XXX

Table 2. Hydrogen Bond Parameters (Å, deg) around the PO_4^{3-} Ion in $[PO_4(L^2)_3]^{3-}$ (5)

N−H···O	N−H	H···O	N···O	∠NHO
N1−H1···O9	0.88	2.13	2.943(7)	153
N2−H2···O8	0.88	1.82	2.700(6)	175
N3−H3···O8	0.88	1.99	2.844(6)	164
N4−H4···O7	0.88	1.97	2.836(7)	168
N5−H5···O9	0.88	2.11	2.942(6)	157
N6−H6···O7	0.88	1.83	2.708(5)	173
N7−H7···O7	0.88	2.04	2.836(6)	150
N8−H8···O10	0.88	1.94	2.820(6)	176
N9−H9···O9	0.88	2.04	2.861(7)	155
N10−H10···O10	0.88	1.85	2.723(6)	173
N11−H11···O10	0.88	1.95	2.812(6)	167
N12−H12···O8	0.88	2.01	2.813(6)	150

phenylene ring, but the total six ethyl groups point to different directions (Figure 5b), possibly due to the small size and flexibility of the alkyl chain. Such arrangements lower the symmetry of complex **5** to C_1.

Thiourea Ligand L^3 and Its Phosphate Complex. The thiourea group has a strong hydrogen-bond donor capability and can form two directional hydrogen bonds with the Y-shaped oxoanions (e.g., carboxylates and phosphates)[22] or chelate spherical anions (e.g., halides[22]) similar to the urea group. However, due to the higher acidity of thiourea than urea (pK_A = 21.1 and 26.9, respectively in DMSO),[23] it is expected that thiourea-containing receptors may establish stronger H-bond interactions and form more stable complexes with anions than their urea counterparts.[24] Thus, we synthesized a bis(thiourea) ligand L^3, which bears two *p*-nitrophenyl terminal substituents (Scheme 1) as in the analogous bisurea ligand L^1.

The free ligand L^3 crystallizes in two distinct structures: L^3·DMSO and L^3·2DMSO. In L^3·DMSO, the ligand molecule assumes a largely bent conformation between the *o*-phenylene spacer and the thiourea groups, which is different from the urea analogue L^1. The two *p*-nitrophenyl groups are almost coplanar (dihedral angle: 6.5°) and are perpendicular to the *o*-phenylene spacer (dihedral angle: 89.3° on average). Notably, each thiourea group adopts an "anti" arrangement; i.e., the two NH groups within one thiourea unit are located in opposite directions (Figure 6a,b). As a result, one of the NH donors of each thiourea (N2, N5) points to the inside of the bent ligand molecule and binds the DMSO, while the other two NH donors turn to the "outside" and one of them (N4) contacts

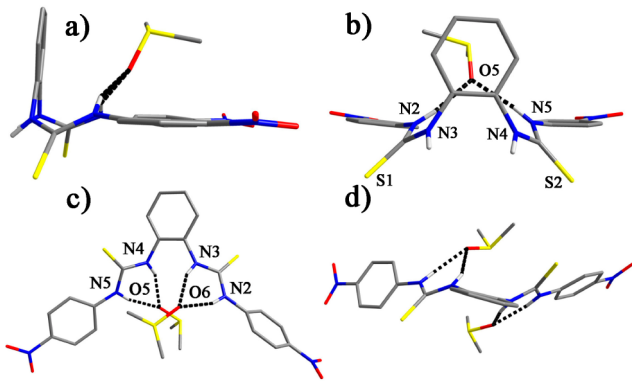

Figure 6. Crystal structures of L^3·DMSO (a, b) and L^3·2DMSO (c, d).

with the thiocarbonyl S (S1) atom from another ligand (N−H···S: 2.66 Å, 134°; Figure S4).

Notably, the ligand conformation in L^3·2DMSO is significantly different from L^3·DMSO. The ligand molecule is more flat than the former one, showing approximately a V-shape. However, the three aryl groups are not coplanar (Figure 6c,d), although the central *o*-phenylene ring does not bend up as in the case of L^3·DMSO. The two thiourea groups assume the normal chelating fashion, and each binds a DMSO molecule above and below the central *o*-phenylene ring, respectively (Figure 6d and Figure S5, Supporting Information). Moreover, both structures are different from the phenyl-substituted analogue reported by Gale et al.,[13] in which one phenyl group is coplanar with the *o*-phenylenediamine spacer but the other phenyl is perpendicular to this plane.

*Phosphate Complex $(TBA)_3[PO_4(L^3)_3]$ (**6**).* When L^3 was treated with TBA_3PO_4 (TBA = tetrabutylammonium) in CH_2Cl_2, golden yellow crystals of the phosphate complex **6** were obtained upon slow vapor diffusion of diethyl ether. Like the analogous urea complex **1**, the structure clearly shows that three ligands coordinate a phosphate ion using all of the six thiourea groups with N···O distances ranging from 3.012 to 2.631 Å (average: 2.806 Å) (Table 3), which are comparable to

Table 3. Hydrogen Bond Parameters (Å, deg) around the PO_4^{3-} Ion in $[PO_4(L^3)_3]^{3-}$ (6)

N−H···O	N−H	H···O	N···O	∠NHO
N2−H2···O15	0.88	1.79	2.645(5)	163
N3−H3···O16	0.88	1.94	2.814(5)	170
N4−H4···O16	0.88	2.03	2.876(5)	162
N5−H5···O13	0.88	1.79	2.653(5)	166
N8−H8···O16	0.88	2.19	2.958(5)	145
N9−H9···O16	0.88	2.03	2.827(5)	150
N10−H10···O14	0.88	2.09	2.912(5)	155
N11−H11···O14	0.88	1.90	2.761(5)	167
N14−H14···O14	0.88	2.11	2.856(5)	142
N15−H15···O15	0.88	1.76	2.631(5)	173
N16−H16···O13	0.88	2.21	3.012(5)	151
N17−H17···O13	0.88	1.87	2.731(5)	166

complex **1** (N···O: 2.935−2.724 Å, 2.809 Å on average). This complex also crystallizes in the space group $P\bar{1}$, and there are two coordination manners for the bis-thiourea ligands, which are also not arranged in the C_3 symmetry. The difference from complex **1** is that three of the thiourea groups chelate the edges and the other three bind the vertices of phosphate ion. The hydrogen bond number on each oxygen atom is also nonequivalent as in **1**. Two oxygen atoms (O13 and O14) accept three hydrogen bonds each, while one oxygen atom (O16) forms four hydrogen bonds and the last one (O15) only two hydrogen bonds (Figure 7a).

Solution Binding Behavior. *^{1}H NMR Studies.* Compared to the free ligand L^1, the ^{1}H NMR spectrum of the phosphate complex **1** showed large downfield shifts ($\Delta\delta$ 2.97−3.24 ppm) of the two NH groups in DMSO-d_6 (Figure 8a). The upfield shifts of H1 and H2 on the terminal aromatic ring (see Scheme 1 for the numbering of protons) induced by the shielding effect provide another evidence for the anion coordination in solution. During the titration of phosphate ions to the ligand in DMSO-d_6−5% H_2O, a new set of signals corresponding to complex **1** appeared when 0.05 equiv of phosphate ions were added. With the addition of more phosphate ions, the peaks of

dx.doi.org/10.1021/ic3028012 | Inorg. Chem. XXXX, XXX, XXX−XXX

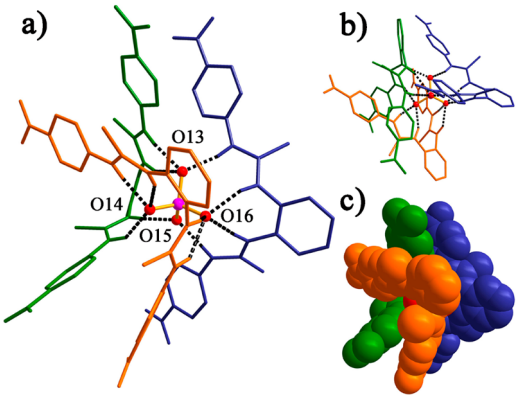

Figure 7. Crystal structure of the phosphate complex $[PO_4(L^3)_3]^{3-}$ (**6**): (a) side view, (b) top view, (c) space-filling representation.

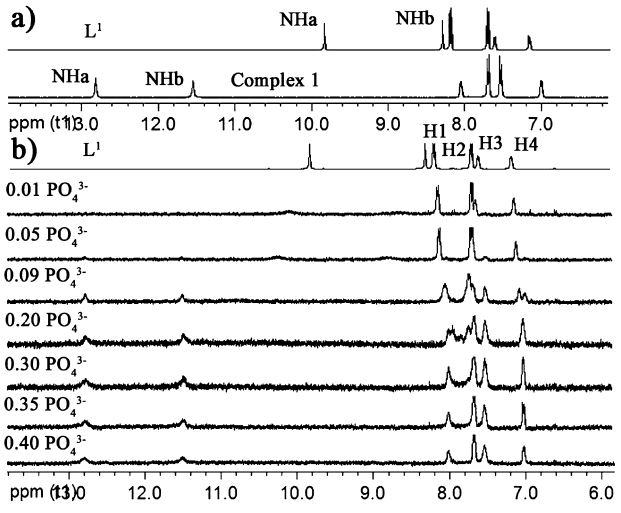

Figure 8. (a) ^{1}H NMR spectra of L^1 and complex **1** in DMSO-d_6. (b) ^{1}H NMR titration of L^1 (5.0×10^{-3} M) with K_3PO_4 in DMSO-d_6–5% H_2O (v/v).

ligand L^1 gradually diminished while the new signals of complex **1** increased. Finally, after addition of ca. 0.35 equiv of phosphate ions, the signals of free L^1 disappeared completely and the new peaks reached saturation, indicating the formation of the 3:1 complex in solution (Figure 8b). However, when more than 1.0 equiv of phosphate anions were added, the NH peaks of complex **1** were broadened again and disappeared gradually with accompanying changes in the aromatic region, which were caused by the through-bond and through-space effects during the deprotonation of ligand L^1 and decomposition of complex **1** (Figure S6).[25] This is consistent with the UV–vis titration results (*vide infra*). Due to the severe broadening and even disappearance of NH signals during the titration process, the association constant for phosphate could not be determined.

In contrast to the slow exchange process observed in the phosphate binding, when L^1 was titrated with SO_4^{2-} (as TBA^+ salt) in DMSO-d_6, a fast exchange occurred. Upon addition of 0.5 equiv of sulfate ions, the spectrum is very close to the 2:1 (host to guest) complex **2** (Figure 9a). The spectrum reached saturation with 1.0 equiv of sulfate ions (Figure 9b), indicating the formation of the 1:1 complex. The saturated downfield shifts of the urea NH signals ($\Delta\delta$ 0.84–1.06 ppm) are much smaller than those for the phosphate ion, implying weaker

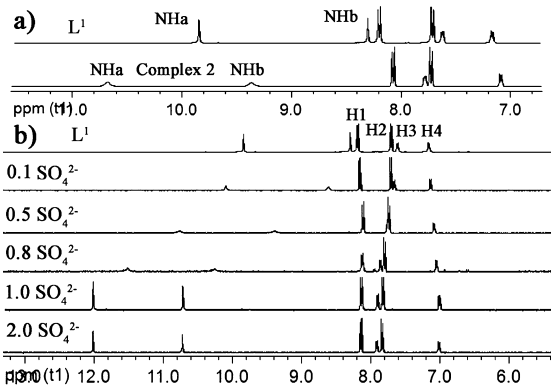

Figure 9. (a) ^{1}H NMR spectra of L^1 and complex **2** in DMSO-d_6. (b) ^{1}H NMR titration of L^1 (5.0×10^{-3} M) with TBA_2SO_4 in DMSO-d_6.

interactions with sulfate. It is noticeable that sulfate ion was bound by less ligands (1:1) in solution than in the solid state (2:1 host to guest), and in both cases the binding stoichiometry is smaller than the phosphate ion (3:1 binding mode both in the solid state and in solution). As mentioned above, this may be attributed to the higher negative charge density and stronger basicity of phosphate ion, and a similar phenomenon has also been observed in our previous work.[10g] The association constant was estimated to be larger than 10^4 M^{-1} for SO_4^{2-} ion by using EQNMR (Table 4, Figure S11).

Table 4. Association Constants (K, M^{-1}) of Ligands L^1 and L^2 with Different Anions[a] from ^{1}H NMR Titrations in DMSO-d_6 at 298 K

anion	PO_4^{3-}	SO_4^{2-}	$H_2PO_4^-$	AcO^-
L^1	*b*	$>10^4$	3090	$>10^4$
L^2	$>10^4$	$>10^4$	2884	1950

[a]Very weak binding for NO_3^- and ClO_4^-. log K could not be determined. Errors <15%. [b]Association constant could not be calculated due to broadening of NMR signals.

Since phosphate and sulfate display different binding modes, competitive experiments between the two anions were carried out both in solution and solid conditions to investigate the selectivity of them. In the NMR studies, when 1.0 equiv of PO_4^{3-} and 1.0 equiv of SO_4^{2-} ions were mixed with L^1 in DMSO-d_6, the spectrum showed mainly the signals of the phosphate complex **1** with only minor amount of the sulfate complex **2** (less than 10%; Figure S7). Moreover, IR spectra and powder X-ray diffraction (PXRD) patterns of the crystals grown from the mixture of L^1, $[K([18]crown-6)]_3PO_4$, TBP_3PO_4, and $[K([18]crown-6)]_2SO_4$ are also close to complex **1**, indicating the preference of L^1 for the phosphate ion (Figures S8, S9). In addition, we have studied the solution binding properties of L^1 with other oxoanions, such as $H_2PO_4^-$, AcO^-, NO_3^-, and ClO_4^-, by ^{1}H NMR titrations. The results demonstrated significant binding affinity of L^1 to $H_2PO_4^-$ and AcO^- ions, with association constants of 3.09×10^3 M^{-1} and $>10^4$ M^{-1}, respectively, while NO_3^- and ClO_4^- showed almost no binding with L^1 (Table 4 and Figures S10–14).

In the case of ligand L^2, the urea NH protons of its phosphate complex **5** displayed smaller downfield shifts ($\Delta\delta$ 1.26–1.97 ppm; Figure S15a) compared to **1**. In the ^{1}H NMR titration experiments, on adding 0.1 equiv of phosphate ions to a solution of L^2, the NH groups experienced some downfield

dx.doi.org/10.1021/ic3028012 | *Inorg. Chem.* XXXX, XXX, XXX–XXX

shifts. However, when more anions were added, the NH signals broadened severely and even disappeared (with 0.3 to 0.5 equiv of PO_4^{3-}), which sharpened again upon addition of ca. 0.7 equiv of PO_4^{3-} ions, and no more changes were observed after addition of 1.0 equiv of anions (Figure S15b). Subsequent Job's plot also demonstrated a binding mode of 1:1 (Figure S16). It can be seen that the diethyl-substituted ligand **L²** displays a much weaker binding affinity than the electron withdrawing nitrophenyl analogue **L¹**, which is reflected not only by the smaller downfield shifts of the NH groups on binding the anion but also by the different binding ratios (1:3 for **L¹** and 1:1 for **L²**).

The binding behavior of **L²** with HCO_3^- (as TEA^+ salt) and CO_3^{2-} (as K^+ salt) ions in solution was also studied. ^{1}H NMR spectrum of the bicarbonate complex **3** showed some downfield shifts for NHa and NHb ($\Delta\delta$ 0.53 and 0.76 ppm) relative to ligand **L²** (Figure S17a). In the titration experiments, the chemical shifts of all of the protons in **L²** kept changing until 2.0 equiv of HCO_3^- ions were added (Figure S17b). The Job's plot revealed a binding mode of 1:2 (host to guest) (Figure S18), with $K_1 = 2.76 \times 10^2$ M^{-1} and $K_2 = 5.97 \times 10^2$ M^{-1} (Figure S19).[26] For the carbonate complex **4**, the downfield shifts of NHa and NHb ($\Delta\delta$ 1.68 and 2.38 ppm) are much larger than those of **3**, indicating a higher affinity (Figure S20a). Upon titration of the anion, NH protons disappeared before the spectrum reached saturation at 1.0 equiv of carbonate ions (Figure S20b), which is consistent with the result of Job's plot (Figure S21), and fitting the titration curve to a 1:1 binding ratio gave an association constant of 1.88×10^3 M^{-1} (Figure S22).

Some other oxoanions (SO_4^{2-}, $H_2PO_4^-$, AcO^-, NO_3^-, and ClO_4^-) were tested in the binding with **L²** by ^{1}H NMR titrations. Job's plots revealed 1:1 stoichiometry for the first three anions (Figure S10), while NO_3^- and ClO_4^- ions were not bound as in the case of **L¹** (Figure S14). The association constants were calculated by EQNMR program, which indicate that **L²** binds PO_4^{3-} and SO_4^{2-} ($K > 10^4$ M^{-1}) more strongly than $H_2PO_4^-$ (2.89×10^3 M^{-1}) and AcO^- (1.95×10^3 M^{-1}) and shows relatively low affinity compared to **L¹** (Table 4; Figures S23–26).

Moreover, ^{1}H NMR titration was also carried out for the bisthiourea ligand **L³**. When 0.1 equiv of PO_4^{3-} ions (as $[K[18]crown\text{-}6)]^+$ salt) were titrated to a solution of **L³** in DMSO-d_6, the NH protons shifted downfield. However, with the increase of phosphate ions (0.2 equiv and more), the NH signals disappeared, and the aromatic region showed gradual appearance of new peaks (Figure S27). Similar phenomena were also observed with other anions (SO_4^{2-}, $H_2PO_4^-$, and AcO^-; Figures S28–30), which may be attributed to the partial deprotonation/decomposition of the bisthiourea in the binding of anions. Thus, the association constants cannot be calculated. The multicomponent equilibria were also proven by the UV–vis titration (vide infra).

UV–Vis Titrations. The anion coordination behavior of **L¹** and **L³**, which bear the nitrophenyl chromophores, with PO_4^{3-}, SO_4^{2-}, $H_2PO_4^-$, AcO^-, NO_3^-, and ClO_4^- (PO_4^{3-} as $[K([18]crown\text{-}6)]^+$ salt and others as TBA^+ salt) was also investigated by UV–vis spectroscopy. Upon titration of these anions, the absorption spectrum of **L¹** exhibited bathochromic shifts except for NO_3^- and ClO_4^- which showed almost no change (Figure S31). With the addition of PO_4^{3-} ions, the absorption band at 352 nm shifted to ca. 363 nm with the appearance of a distinct isosbestic point and slowly reached a plateau on addition of ca. 0.35 equiv. of PO_4^{3-} ions (Figure S31a). The fitting curve at 360 nm also revealed a 3:1 (H/G) binding mode that is consistent with the solid-state structure. When sulfate ions were added to the solution of **L¹**, a red shift of ca. 18 nm was observed with an isosbestic point at 356 nm. However, the plateau was reached after the addition of 1.0 equiv of the anion (Figure S31b), indicating a binding mode of 1:1 in solution, which is different from the crystal structure (2:1 H/G). For $H_2PO_4^-$ and AcO^- ions, the binding mode obtained from UV–vis (Figure S31c,d) is in good agreement with the ^{1}H NMR titration.[27] It is worth noting that, when large amounts of PO_4^{3-} ions were added to the solution of **L¹**, a new band at ca. 475 nm emerged with accompanying decrease of the absorbance at 375 nm and appearance of an isosbestic point at ca. 411 nm, demonstrating the deprotonation of **L¹** ligand (Figure S32).[11c,25b] For the thiourea receptor **L³**, the titration profiles either displayed more than one isosbestic points (for PO_4^{3-} and SO_4^{2-}) or kept changing (for $H_2PO_4^-$ and AcO^-) with the addition of anions, which provide another evidence for the decomposition of **L³** in the presence of anions (Figure S33).

CONCLUSION

The coordination behavior of bisurea (**L¹** and **L²**) and bisthiourea (**L³**) ligands with the phosphate anion was studied both in the solid state and in solution. The three ligands can readily form the tris-chelate complexes $[(PO_4)L_3]^{3-}$ (**1**, **5**, **6**) with orthophosphate ion in the solid state, in which the anion is coordinated by six urea groups through 12 hydrogen bonds (the saturated coordination of tetrahedral anion). The structure of these complexes can be viewed as the counterpart of the well-known $[M(bpy)_3]^{n+}$ complexes, thus providing further evidence for the resemblance between anion coordination and transition-metal coordination. However, the coordination number in solution is different from the solid state. Although ligand **L¹** shows the 3:1 binding ratio with phosphate ion in solution, the diethyl-substituted analogue **L²** forms only the 1:1 complex, which can be attributed to the weaker hydrogen bonding affinity of **L²** due to the lack of electron-withdrawing substituents. The thiourea ligand **L³**, on the other hand, exhibits the typical deprotonation with basic anions. The results once again demonstrated the strong tendency of phosphate ion to form 12 hydrogen bonds in the solid state, which makes a promising coordination center to oligoureas.

EXPERIMENTAL SECTION

General. 1,2-Phenylenediamine, *p*-nitrophenyl isocyanate, and ethyl isocyanate were purchased from Alfa Aesar and used as received. All solvents and other reagents were of reagent grade quality. Ligand **L¹** was synthesized following the literature procedures.[13] ^{1}H and ^{13}C NMR spectra were recorded on a Mercury plus-400 spectrometer at 400 and 100 MHz, respectively, using TMS as an internal standard. UV–vis spectra were performed on an HP8453 spectrophotometer (1 cm quartz cell). Elemental analyses were performed on an Elementar VarioEL instrument. IR spectra were recorded on a Bruker IFS 120HR spectrometer. ESI-MS measurements were carried out using a Waters ZQ4000 spectrometer. Melting points were detected on an X-4 Digital Vision MP Instrument.

Synthesis of Ligands L², L³ and the Anion Complexes 1–6. For **L²**, a solution of 1,2-phenylenediamine (0.324 g, 3 mmol) in 120 mL of THF was added dropwise to a solution of ethyl isocyanate (665 μL, 8.4 mmol) in CH_2Cl_2 (100 mL). After refluxing under stirring for 24 h, the precipitate was filtered off and washed several times with THF and diethyl ether and then recrystallized from CH_2Cl_2/DMSO

dx.doi.org/10.1021/ic3028012 | Inorg. Chem. XXXX, XXX, XXX–XXX

(v/v 40:1) by diffusion of hexane to yield $\mathbf{L}^2$ as a white solid (0.644 g, 70%). Mp: 189 °C. ^{1}H NMR (400 MHz, DMSO-d_6, ppm): 7.75 (s, 2H, Ha), 7.45 (m, 2H, H3), 6.95 (m, 2H, H4), 6.48 (t, J = 5.6 Hz, 2H, Hb), 3.10 (m, 4H, H2), 1.05 (t, J = 5.2 Hz, 6H, H1). ^{13}C NMR (100 MHz, DMSO-d_6): 155.7 (C), 131.5 (C), 123.4 (CH), 123.1 (CH), 34.1 (CH_2), 15.4 (CH_3). IR (KBr, ν/cm^{-1}): 3319, 2974, 2930, 1636, 1551, 1567, 1481, 1454, 757. Anal. Calcd for $C_{12}H_{18}N_4O_2$: C, 57.58; H, 7.25; N, 22.38%. Calcd for $C_{12}H_{18}N_4O_2{\cdot}0.2C_4H_8O$: C, 58.08; H, 7.46; N, 21.16%. Found: C, 57.65; H, 7.00; N, 21.37%. ESI-MS: m/z 249.14 $[M-H]^-$; 285.14 $[M + Cl]^-$.

For $\mathbf{L}^3$, A solution of 1,2-phenylenediamine (0.114 g, 1.06 mmol) in 20 mL of THF was added dropwise to a solution of *p*-nitrophenylisothiocyanate (0.576 g, 3.20 mmol) in THF (20 mL). After refluxing under stirring for 36 h, the precipitate was filtered off and washed several times with THF and diethyl ether and then dried in vacuum to yield $\mathbf{L}^3$ as a yellow solid (248 mg, 50%). Mp: 176 °C. ^{1}H NMR (400 MHz, DMSO-d_6, ppm): 10.61 (s, 2H, Ha), 9.65 (s, 2H, Hb), 8.18 (d, J = 9.2 Hz, 4H, H4), 7.88 (d, J = 9.2 Hz, 4H, H3), 7.53 (m, 2H, H2), 7.32 (m, 2H, H1). ^{13}C NMR (100 MHz, DMSO-d_6): 179.9 (C), 145.9 (C), 142.4 (C), 134.0 (C), 128.1 (CH), 126.7 (CH), 124.3 (CH), 121.5 (CH). IR (KBr, ν/cm^{-1}): 3221, 3104, 2963, 1528, 1510, 1298, 1178, 1110, 854. Anal. Calcd for $C_{20}H_{16}N_6O_4S_2{\cdot}2$DMSO: C, 46.14; H, 4.52; N, 13.45%. Found: C, 46.47; H, 4.15; N, 12.86%. ESI-MS: m/z 467.03 $[M-H]^-$, 504.01 $[M + Cl]^-$.

[K([18]crown-6)]$_2$(TBP)[PO$_4$(L^1)$_3$] (1). $\mathbf{L}^1$ (19.6 mg, 0.045 mmol), K_3PO_4 (3 mg, 0.015 mmol), [18]crown-6 (14 mg, 0.045 mmol), and tetrabutylphosphonium phosphate (generated from TBPOH and H_3PO_4, 0.015 mmol) were suspended in acetone (2 mL). After stirring for 1 h at room temperature, a clear yellow solution was obtained. Slow vapor diffusion of diethyl ether into this solution afforded yellow crystals of complex **1** within 1 day (22 mg, 65%). Mp: 160 °C. Anal. Calcd for $C_{100}H_{132}K_2N_{18}O_{34}P_2$: C, 52.90; H, 5.86; N, 11.10%. Found: C, 52.82; H, 5.78; N, 11.08%.

[K([18]crown-6)]$_2$[SO$_4$(L^1)$_2$]·C$_3$H$_6$O (2). $\mathbf{L}^1$ (19.6 mg, 0.045 mmol), K_2SO_4 (3 mg, 0.015 mmol), and [18]crown-6 (14 mg, 0.045 mmol) were suspended in mixed solvents of acetone (2 mL) and DMSO (200 μL). After stirring for 1 h at room temperature, a clear yellowish solution was obtained. Slow vapor diffusion of diethyl ether afforded yellow crystals within 1 day (20 mg, 55%). Mp: 204 °C. Anal. Calcd for $C_{67}H_{86}K_2N_{12}O_{29}S$: C, 49.26; H, 5.31; N, 10.29%. Found: C, 48.92; H, 5.04; N, 10.71%.

[K([18]crown-6)]·[(HCO$_3$)(L^2)] (3). $\mathbf{L}^2$ (11.2 mg, 0.045 mmol), K_3PO_4 (3 mg, 0.015 mmol), and [18]crown-6 (14 mg, 0.045 mmol) were suspended in acetone/water (2 mL, 40:1 v/v) and stirred for 1 h at room temperature to give a clear colorless solution. Slow vapor diffusion of diethyl ether afforded colorless crystals within 1 day (5.5 mg, 20%). Mp: 133 °C. Anal. Calcd for $C_{25}H_{43}KN_4O_{11}$: C, 48.85; H, 7.05; N, 9.11%. Found: C, 48.94; H, 6.71; N, 8.62%. ESI-MS: m/z 311.14 $[M + HCO_3]^-$.

(TEA)$_2$[(CO$_3$)(L^2)$_2$] (4). $\mathbf{L}^2$ (11.2 mg, 0.045 mmol) and $TEAHCO_3$ (11.2 mg, 0.045 mmol) were suspended in acetone and stirred for 10 min at room temperature to give a clear colorless solution. Slow vapor diffusion of diethyl ether afforded colorless crystals within 1 day (11.1 mg, 60%). Mp: 182 °C. Anal. Calcd for $C_{41}H_{76}N_{10}O_7$: C, 59.97; H, 9.33; N, 17.06%. Found: C, 59.85; H, 9.05; N, 16.82%.

(TMA)$_3$[PO$_4$(L^2)$_3$]·4H$_2$O (5). $\mathbf{L}^2$ (11.2 mg, 0.045 mmol) was reacted with $(TMA)_3PO_4$ (generated from (TMA)OH and H_3PO_4, 0.015 mmol) in acetonitrile (2 mL). A clear colorless solution was obtained soon. Slow vapor diffusion of diethyl ether afforded colorless crystals within 1 day (10 mg, 62%). Mp: 173 °C. Anal. Calcd for $(TMA)_3[PO_4(L^2)_3]{\cdot}7H_2O$ ($C_{48}H_{104}N_{15}O_{17}P$): C, 48.27; H, 8.78; N, 17.59%. Found: C, 48.55; H, 8.36; N, 17.43%.

(TBA)$_3$[PO$_4$(L^3)$_3$] (6). $\mathbf{L}^3$ (10.5 mg, 0.0225 mmol) was reacted with $(TBA)_3PO_4$ (generated from (TBA)OH and $(TBA)H_2PO_4$, 0.0075 mmol) in CH_2Cl_2 (1 mL). A clear orange solution was obtained soon. Slow vapor diffusion of diethyl ether afforded golden yellow crystals within 1 day (6.7 mg, 40%). Mp: 121 °C. Anal. Calcd for $(TBA)_3[PO_4(L^3)_3]{\cdot}H_2O$ ($C_{108}H_{158}N_{21}O_{17}PS_6$): C, 57.76; H, 7.09; N, 13.10%. Found: C, 58.08; H, 6.82; N, 12.47%.

X-ray Crystallography. Diffraction data were collected on a Bruker SMART APEX II diffractometer at 150 K with graphite-monochromated Mo Kα radiation (λ = 0.710 73 Å). An empirical absorption correction using SADABS was applied for all data. The structures were solved by direct methods using the SHELXS program. All non-hydrogen atoms were refined anisotropically by full-matrix least-squares on F^2 by the use of the SHELXL program. Hydrogen atoms bonded to carbon and nitrogen were included in idealized geometric positions with thermal parameters equivalent to 1.2 times those of the atom to which they were attached. Some residual peaks around $[K([18]crown-6)]^+$ and TBP^+ in complex **1** were squeezed due to severe thermal vibration, and the disordered solvents were also squeezed.

Crystal Data for L^1. $C_{23}H_{19}N_6O_8S$ (539.50), yellow block, orthorhombic, space group $P2_12_12_1$, a = 4.433(2) Å, b = 20.900(11) Å, c = 30.555(16) Å, V = 2831(3) Å^3, T = 153(2) K, Z = 4, D_{calcd} = 1.266 g cm^{-3}, F_{000} = 1116, μ = 0.168 mm^{-1}, 18 803 reflections collected, 4996 unique (R_{int} = 0.0494), no. of observed reflections 3447 [$I > 2\sigma(I)$]; R1 = 0.0699, wR2 = 0.2065 [$I > 2\sigma(I)$].

Crystal Data for L^3·DMSO. $C_{22}H_{22}N_6O_5S_3$ (546.64), yellow block, monoclinic, space group $P2_1/c$, a = 18.144(7) Å, b = 9.602(4) Å, c = 14.162(6) Å, β = 90.816(6)°, V = 2466.9(17) Å^3, T = 153(2) K, Z = 4, D_{calcd} = 1.472 g cm^{-3}, F_{000} = 1136, μ = 0.347 mm^{-1}, 15 544 reflections collected, 4362 unique (R_{int} = 0.0686), no. of observed reflections 3120 [$I > 2\sigma(I)$]; R1 = 0.0482, wR2 = 0.0924 [$I > 2\sigma(I)$].

Crystal Data for L^3·2DMSO. $C_{24}H_{28}N_6O_6S_4$ (624.76), yellow block, monoclinic, space group $P2_1/n$, a = 13.657(8) Å, b = 12.406(7) Å, c = 17.445(10) Å, β = 90.859(8)°, V = 2955(3) Å^3, T = 153(2) K, Z = 4, D_{calcd} = 1.404 g cm^{-3}, F_{000} = 1304, μ = 0.370 mm^{-1}, 19 184 reflections collected, 5122 unique (R_{int} = 0.0402), no. of observed reflections 2965 [$I > 2\sigma(I)$]; R1 = 0.0936, wR2 = 0.1612 [$I > 2\sigma(I)$].

Crystal Data for 1. $C_{100}H_{132}K_2N_{18}O_{34}P_2$ (2270.38), yellow block, triclinic, space group $P\bar{1}$, a = 15.349(3) Å, b = 17.380(4) Å, c = 25.465(5) Å, α = 109.489(2)°, β = 106.656(3)°, γ = 90.163(3)°, V = 6099(2) Å^3, T = 153(2) K, Z = 2, D_{calcd} = 1.236 g cm^{-3}, F_{000} = 2396, μ = 0.184 mm^{-1}, 40 494 reflections collected, 21 027 unique (R_{int} = 0.0358), no. of observed reflections 149 21 [$I > 2\sigma(I)$]; R1 = 0.1099, wR2 = 0.2166 [$I > 2\sigma(I)$].

Crystal Data for 2. $C_{67}H_{86}K_2N_{12}O_{29}S$ (1633.74), yellow block, triclinic, space group $P\bar{1}$, a = 12.0010(9) Å, b = 15.0158(12) Å, c = 22.8150(18) Å, α = 85.9980(10)°, β = 86.3910(10)°, γ = 71.3080(10)°, V = 3881.4(5) Å^3, T = 153(2) K, Z = 2, D_{calcd} = 1.398 g cm^{-3}, F_{000} = 1716, μ = 0.239 mm^{-1}, 25 841 reflections collected, 13 410 unique (R_{int} = 0.0226), no. of observed reflections 11 455 [$I > 2\sigma(I)$]; R1 = 0.0379, wR2 = 0.0839 [$I > 2\sigma(I)$].

Crystal Data for 3. $C_{25}H_{43}KN_4O_{11}$ (614.73), colorless block, triclinic, space group $P\bar{1}$, a = 8.3476(7) Å, b = 11.1908(10) Å, c = 16.6700(15) Å, α = 87.8650(10)°, β = 85.2360(10)°, γ = 77.4120(10)°, V = 1514.3(2) Å^3, T = 153(2) K, Z = 2, D_{calcd} = 1.348 g cm^{-3}, F_{000} = 656, μ = 0.238 mm^{-1}, 10 012 reflections collected, 5205 unique (R_{int} = 0.0174), no. of observed reflections 4463 [$I > 2\sigma(I)$]; R1 = 0.0351, wR2 = 0.0830 [$I > 2\sigma(I)$].

Crystal Data for 4. $C_{41}H_{76}N_{10}O_7$ (821.12), colorless block, monoclinic, space group $P2_1/n$, a = 9.123(2) Å, b = 20.426(5) Å, c = 13.377(4) Å, β = 107.893(3)°, V = 2372.1(11) Å^3, T = 153(2) K, Z = 2, D_{calcd} = 1.150 g cm^{-3}, F_{000} = 896, μ = 0.079 mm^{-1}, 15 911 reflections collected, 4277 unique (R_{int} = 0.0269), no. of observed reflections 2515 [$I > 2\sigma(I)$]; R1 = 0.0924, wR2 = 0.1540 [$I > 2\sigma(I)$].

Crystal Data for 5. $C_{48}H_{98}N_{15}O_{14}P$ (1140.38), colorless block, monoclinic, space group Cc, a = 24.135(6) Å, b = 13.340(3) Å, c = 22.620(9) Å, β = 112.186(3)°, V = 6744(3) Å^3, T = 153(2) K, Z = 4, D_{calcd} = 1.123 g cm^{-3}, F_{000} = 2472, μ = 0.105 mm^{-1}, 21 488 reflections collected, 11 628 unique (R_{int} = 0.0418), no. of observed reflections 7482 [$I > 2\sigma(I)$]; R1 = 0.0772, wR2 = 0.1669 [$I > 2\sigma(I)$].

Crystal Data for 6. $C_{108}H_{156}N_{21}O_{16}PS_6$ (2227.87), yellow block, triclinic, space group $P\bar{1}$, a = 18.1963(16) Å, b = 18.2842(16) Å, c = 22.399(2) Å, α = 77.7590(10)°, β = 72.8240(10)°, γ = 61.7220(10)°, V = 6247.1(10) Å^3, T = 153(2) K, Z = 2, D_{calcd} = 1.184 g cm^{-3}, F_{000} = 2380, μ = 0.188 mm^{-1}, 40 116 reflections collected, 21 028 unique

dx.doi.org/10.1021/ic3028012 | Inorg. Chem. XXXX, XXX, XXX–XXX

(R_{int} = 0.0352), no. of observed reflections 13 777 [$I > 2\sigma(I)$]; R1 = 0.0846, wR2 = 0.1788 [$I > 2\sigma(I)$].

^{1}H NMR Titration. Stock solutions of **L** (**L** = **L^1**, **L^2**, **L^3**) (1.0×10^{-2} M) in DMSO-d_6 (0.5 mL), $[K([18]crown\text{-}6)]_3PO_4$, and $[K([18]crown\text{-}6)]_2CO_3$ in H_2O (0.3 mL, 0.25 M) and TBA_2SO_4, $TEAHCO_3$ in DMSO-d_6 (0.3 mL, 0.25 M) were prepared for the ^{1}H NMR titrations. Small portions (2−10 μL) of the anion solution were added to the solution of ligand **L** (DMSO-d_6), and the spectrum was recorded after each addition.

^{1}H NMR Job's Plot. Stock solutions of host (5.0 mM) and guest (5.0 mM) in DMSO-d_6 (5.0 mL) were prepared in separate volumetric flasks. The 5 mm-o.d. NMR tubes were separately filled with a total of 500 μL solution of the host and guest in the following ratios (μL, host/guest) at 297 K: 10:0, 9:1, 8:2, 7:3, 6:4, 5:5, 4:6, 3:7, 2:8, 1:9. The ^{1}H NMR spectra were obtained for each tube, and the H3 and H4 signals were used to calculate the complex concentration, $[HG] = [H]_t \times (\delta_{obsd} - \delta_{free})/(\delta_{com} - \delta_{free})$, where $[H]_t$ is the total concentration of the host, δ_{obsd} is the chemical shift observed on every point, and δ_{free} and δ_{com} correspond to the chemical shifts of the free ligand and the complex. This value was plotted against the molar fraction of the host. The association constants (K's) were determined by EQNMR.[26]

UV−Vis Titration. Stock solutions of **L** (**L** = **L^1**, **L^3**) (2.0×10^{-2} M) in DMSO (1 mL) and K_3PO_4 (4×10^{-3} M) in H_2O (1 mL) were prepared for the UV−vis titrations. Small portions (2−4 μL) of the anion solution were added to the solution of ligand **L** (2.0 μL in 2.0 mL DMSO−5% H_2O), and the spectrum was recorded after each addition.

■ ASSOCIATED CONTENT

Ⓢ Supporting Information

Additional crystal structures and hydrogen bonding parameters, IR spectra of the complexes, ^{1}H NMR and UV−vis titrations, and detailed information of the X-ray crystal structure analysis of compounds **1**−**6** (CIF). This material is available free of charge via the Internet at http://pubs.acs.org.

■ AUTHOR INFORMATION

Corresponding Author

*E-mail: wubiao@nwu.edu.cn.

Notes

The authors declare no competing financial interest.

■ ACKNOWLEDGMENTS

This work was supported by the National Natural Science Foundation of China (Grant 21271149).

■ REFERENCES

(1) (a) Steed, J. W.; Atwood, J. L. *Supramolecular Chemistry*. John Wiley & Sons, Ltd.: New York, 2009. (b) Sessler, J. L.; Gale, P. A.; Cho, W.-S. *Anion Receptor Chemistry*; Royal Society of Chemistry: Cambridge, U.K., 2006. (c) Lehn, J.-M. *Supramolecular Chemistry: Concepts and Perspectives*; VCH: Weinheim: 1995. (d) Gale, P. A. *Acc. Chem. Res.* **2006**, *39*, 465−475. (e) Katayev, E. A.; Ustynyuk, Y. A.; Sessler, J. L. *Coord. Chem. Rev.* **2006**, *250*, 3004−3037. (f) Gale, P. A.; García-Garrido, S. E.; Garric, J. *Chem. Soc. Rev.* **2008**, *37*, 151−190. (g) Gale, P. A.; García-Garrido, S. E.; Garric, J. *Chem. Soc. Rev.* **2008**, *37*, 151−190. (h) Caltagirone, C.; Gale, P. A. *Chem. Soc. Rev.* **2009**, *38*, 520−563. (i) Steed, J. W. *Chem. Soc. Rev.* **2009**, *38*, 506−519. (j) Gale, P. A. *Chem. Soc. Rev.* **2010**, *39*, 3746−3771. (k) Wenzel, M.; Hiscock, J. R.; Gale, P. A. *Chem. Soc. Rev.* **2012**, *41*, 480−520.

(2) (a) Lehn, J.-M. *Acc. Chem. Res.* **1978**, *11*, 49−57. (b) Lehn, J. M. *Pure Appl. Chem.* **1978**, *50*, 871−892.

(3) (a) Atwood, J. L.; Steed, J. W. *Supramolecular Chemistry of Anions*; VCH: Weinheim, 1997. (b) Bowman-James, K. *Acc. Chem. Res.* **2005**, *38*, 671−678. (c) Kang, S. O.; Begum, R. A.; Bowman-James, K. *Angew. Chem., Int. Ed.* **2006**, *45*, 7882−7894. (d) Bowman-James, K.; Bianchi, A.; García-España, E. *Anion Coordination Chemistry*; Wiley VCH: Weinheim, 2011.

(4) (a) Juris, A.; Barigelletti, S.; Campagna, S.; Balzani, V.; Belser, P.; von Zelewsky, A. *Coord. Chem. Rev.* **1988**, *84*, 85−277. (b) Reedijk, J.; Wilkinson, S. G.; Gillard, R. D.; McCleverty, J. A.; Press, P. *Comprehensive Coordination Chemistry*; Oxford University Press: Oxford, U.K., 1987. (c) Constable, E. C.; Steel, P. J. *Coord. Chem. Rev.* **1989**, *93*, 205−223. (d) Kaes, C.; Katz, A.; Hosseini, M. W. *Chem. Rev.* **2000**, *100*, 3553−3590. (e) Constable, E. C. *Comprehensive Supramolecular Chemistry*; Pergamon: Oxford, U.K., 1996. (f) Sauvage, J. P. *Transition Metals in Supramolecular Chemistry*; Wiley: New York, 1999.

(5) Piguet, C.; Bernardinelli, G.; Hopfgartner, G. *Chem. Rev.* **1997**, *97*, 2005−2062.

(6) (a) Knof, U.; von Zelewsky, A. *Angew. Chem., Int. Ed.* **1999**, *38*, 302−322. (b) Belser, P.; Bernhard, S.; Jandrasics, E.; von Zelewsky, A.; De Cola, L.; Balzani, V. *Coord. Chem. Rev.* **1997**, *159*, 11.

(7) (a) Balzani, V.; Juris, A.; Venturi, M.; Campagna, S.; Serroni, S. *Chem. Rev.* **1996**, *96*, 759−833. (b) Ward, M. D.; White, C. M.; Barigelletti, F.; Armaroli, N.; Calogero, G.; Flamigni, L. *Coord. Chem. Rev.* **1998**, *171*, 481−488.

(8) (a) Kalyanasundaram, K.; Grätzel, M. *Coord. Chem. Rev.* **1998**, *177*, 347−414. (b) Baxter, S. M.; Jones, W. E., Jr.; Danielson, E.; Worl, L.; Strouse, G.; Younathan, J.; Meyer, T. J. *Coord. Chem. Rev.* **1991**, *111*, 47−71.

(9) Venturi, M.; Credi, A.; Balzani, V. *Coord. Chem. Rev.* **1999**, *186*, 233−256.

(10) (a) Wu, B.; Liang, J.; Yang, J.; Jia, C.; Yang, X.-J.; Zhang, H.; Tang, N.; Janiak, C. *Chem. Commun.* **2008**, 1762−1764. (b) Jia, C.; Wu, B.; Li, S.; Huang, X.; Yang, X.-J. *Org. Lett.* **2010**, *12*, 5612−5615. (c) Jia, C.; Wu, B.; Li, S.; Yang, Z.; Zhao, Q.; Liang, J.; Li, Q.-S.; Yang, X.-J. *Chem. Commun.* **2010**, *46*, 5376−5378. (d) Jia, C.; Wu, B.; Li, S.; Huang, X.; Zhao, Q.; Li, Q.-S.; Yang, X.-J. *Angew. Chem., Int. Ed.* **2011**, *50*, 486−490. (e) Li, S.; Jia, C.; Wu, B.; Luo, Q.; Huang, X.; Yang, Z.; Li, Q.-S.; Yang, X.-J. *Angew. Chem., Int. Ed.* **2011**, *50*, 1−5. (f) Yang, Z.; Wu, B.; Huang, X.; Liu, Y.; Li, S.; Xia, Y.; Jia, C.; Yang, X.-J. *Chem. Commun.* **2011**, *47*, 2880−2882. (g) Li, S.; Wei, M.; Huang, X.; Yang, X.-J.; Wu, B. *Chem. Commun.* **2012**, *48*, 3097−3099. (h) Wu, B.; Jia, C.; Wang, X.; Li, S.; Huang, X.; Yang, X.-J. *Org. Lett.* **2012**, *14*, 684−687.

(11) (a) Dydio, P.; Zielinski, T.; Jurczak, J. *Chem. Commun.* **2009**, 4560−4562. (b) Kondo, S.-i.; Hiraoka, Y.; Kurumatani, N.; Yano, Y. *Chem. Commun.* **2005**, 1720−1722. (c) Odago, M. O.; Colabello, D. M.; Lees, A. J. *Tetrahedron* **2010**, *66*, 7465−7471.

(12) Caltagirone, C.; Hiscock, J. R.; Hursthouse, M. B.; Light, M. E.; Gale, P. A. *Chem.—Eur. J.* **2008**, *14*, 10236−10243.

(13) Brooks, S. J.; Edwards, P. R.; Gale, P. A.; Light, M. E. *New J. Chem.* **2006**, *30*, 65−70.

(14) Bryantsev, V. S.; Hay, B. P. *J. Am. Chem. Soc.* **2006**, *128*, 2035−2042.

(15) (a) Moore, S. J.; Haynes, C. J. E.; González, J.; Sutton, J. L.; Brooks, S. J.; Light, M. E.; Herniman, J.; Langley, G. J.; Soto-Cerrato, V.; Pérez-Tomás, R.; Marque, I.; Costa, P. J.; Félix, V.; Gale, P. A. *Chem. Sci.* **2013**, *4*, 103−117. (b) Brooks, S. J.; Gale, P. A.; Light, M. E. *CrystEngComm* **2005**, *7*, 586−591. (c) Brooks, S. J.; Gale, P. A.; Light, M. E. *Chem. Commun.* **2005**, 4696−4698.

(16) Amendola, V.; Boiocchi, M.; Esteban-Gómez, D.; Fabbrizzi, L.; Monzani, E. *Org. Biomol. Chem.* **2005**, *3*, 2632−2639.

(17) Hay, B. P.; Firman, T. K.; Moyer, B. A. *J. Am. Chem. Soc.* **2005**, *127*, 1810−1819.

(18) (a) Custelcean, R.; Moyer, B. A.; Hay, B. P. *Chem. Commun.* **2005**, 5971−5973. (b) Custelcean, R.; Remy, P.; Bonnesen, P. V.; Jiang, D.-e.; Moyer, B. A. *Angew. Chem., Int. Ed.* **2008**, *47*, 1866−1870. (c) Custelcean, R.; Bosano, J.; Bonnesen, P. V.; Kertesz, V.; Hay, B. P. *Angew. Chem., Int. Ed.* **2009**, *48*, 4025−4029. (d) Ravikumar, I.; Lakshminarayanan, P. S.; Arunachalam, M.; Suresh, E.; Ghosh, P. *Dalton Trans.* **2009**, 4160−4168. (e) Yi, S.; Brega, V.; Captaina, B.; Kaifer, A. E. *Chem. Commun.* **2012**, *48*, 10295−10297.

(19) (a) Zhuge, F.; Wu, B.; Liang, J.; Yang, J.; Liu, Y.; Jia, C.; Janiak, C.; Tang, N.; Yang, X.-J. *Inorg. Chem.* **2009**, *48*, 10249−10256. (b) Jose, D. A.; Kumar, D. K.; Ganguly, B.; Das, A. *Inorg. Chem.* **2007**, *46*, 5817−5819. (c) Pflugrath, J. W.; Quiocho, F. A. *Nature* **1985**, *314*, 257−260. (d) Custelcean, R.; Sellin, V.; Moyer, B. A. *Chem. Commun.* **2007**, 1541−1543. (e) Gale, P. A.; Hiscock, J. R.; Jie, C. Z.; Hursthouse, M. B.; Light, M. E. *Chem. Sci.* **2010**, *1*, 215−220. (f) Kim, J.-i.; Juwarker, H.; Liu, X.; Lah, M. S.; Jeong, K.-S. *Chem. Commun.* **2010**, *46*, 764−766. (g) Mendy, J. S.; Pilate, M. L.; Horne, T.; Day, V. W.; Hossain, M. A. *Chem. Commun.* **2010**, *46*, 6084−6086.

(20) (a) Busschaert, N.; Wenzel, M.; Light, M. E.; Iglesias-Hernández, P.; Pérez-Tomás, R.; Gale, P. A. *J. Am. Chem. Soc.* **2011**, *133*, 14136−14148. (b) Ravikumar, I.; Ghosh, P. *Chem. Commun.* **2010**, *46*, 6741−6743. (c) Wei, M.; Wu, B.; Zhao, L.; Zhang, H.; Li, S.; Zhao, Y.; Yang, X.-J. *Org. Biomol. Chem.* **2012**, *10*, 8758−8761. (d) Brooks, S. J.; Gale, P. A.; Light, M. E. *Chem. Commun.* **2006**, 4344−4346. (e) Gunnlaugsson, T.; Kruger, P. E.; Jensen, P.; Pfeffer, F. M.; Hussey, G. M. *Tetrahedron Lett.* **2003**, *44*, 8909−8913. (f) Ravikumar, I.; Ghosh, P. *Chem. Commun.* **2010**, *46*, 1082−1084.

(21) Quinn, R.; Appleby, J. B.; Pez, G. P. *J. Am. Chem. Soc.* **1995**, *117*, 329−335.

(22) (a) Costero, A. M.; Gaviña, P.; Rodríguez-Muñiz, G. M.; Gil, S. *Tetrahedron* **2007**, *63*, 7899−7905. (b) Al-Sayaha, M. H.; Branda, N. R. *Thermochim. Acta* **2010**, *503*−*504*, 28−32. (c) Pfeffer, F. M.; Kruger, P. E.; Gunnlaugsson, T. *Org. Biomol. Chem.* **2007**, *5*, 1894−1902. (d) Pfeffer, F. M.; Gunnlaugsson, T.; Jensen, P.; Kruger, P. E. *Org. Lett.* **2005**, *7*, 5357−5360. (e) Duke, R. M.; Gunnlaugsson, T. *Tetrahedron Lett.* **2007**, *48*, 8043−8047. (f) Liu, S. Y.; Law, K. Y.; He, Y. B.; Chan, W. H. *Tetrahedron Lett.* **2006**, *47*, 7857−7860.

(23) Bordwell, F. G.; Algrim, D.; Harrelson, J. A., Jr. *J. Am. Chem. Soc.* **1988**, *110*, 5904−5906.

(24) (a) Nishizawa, S.; Bühlmann, P.; Iwao, M.; Umezawa, Y. *Tetrahedron Lett.* **1995**, *36*, 6483−6486. (b) Fan, E.; Arman, S. A. V.; Kincaid, S.; Hamilton, A. D. *J. Am. Chem. Soc.* **1993**, *11*, 369−370.

(25) (a) Gómez, D. E.; Fabbrizzi, L.; Licchelli, M.; Monzani, E. *Org. Biomol. Chem.* **2005**, *3*, 1495−1500. (b) Boiocchi, M.; Boca, L. D.; Gómez, D. E.; Fabbrizzi, L.; Licchelli, M.; Monzani, E. *J. Am. Chem. Soc.* **2004**, *126*, 16507−16514. (c) Jia, C.; Wu, B.; Liang, J.; Huang, X.; Yang, X.-J. *J. Fluor.* **2010**, *20*, 291−297. (d) Duke, R. M.; O'Brien, J. E.; McCabe, T.; Gunnlaugsson, T. *Org. Biomol. Chem.* **2008**, *6*, 4089−4092.

(26) Hynes, M. J. *J. Chem. Soc., Dalton Trans.* **1993**, 311−312.

(27) Boyle, E. M.; McCabe, T.; Gunnlaugsson, T. *Supramol. Chem.* **2010**, *22*, 586−597.